

OPEN ACCESS

EDITED BY

Honglei Wang,

Nanjing University of Information Science and Technology, China

REVIEWED BY

Yuhan Wang, Stanford University, United States Yan Xiang, Anhui University, China

*CORRESPONDENCE

RECEIVED 03 October 2025 REVISED 08 November 2025 ACCEPTED 11 November 2025 PUBLISHED 19 November 2025

CITATION

Yang T, Tian Y and Wang Z (2025) Unveiling the critical role of tall-stack emissions in winter nitrate episodes over North China through machine learning and 3D model analysis. Front. Environ. Sci. 13:1718020. doi: 10.3389/fenvs.2025.1718020

COPYRIGHT

© 2025 Yang, Tian and Wang. This is an openaccess article distributed under the terms of the Creative Commons Attribution License (CC BY). The use, distribution or reproduction in other forums is permitted, provided the original author(s) and the copyright owner(s) are credited and that the original publication in this journal is cited, in accordance with accepted academic practice. No use, distribution or reproduction is permitted which does not comply with these terms.

Unveiling the critical role of tall-stack emissions in winter nitrate episodes over North China through machine learning and 3D model analysis

Ting Yang^{1*}, Yutong Tian^{1,2} and Zifa Wang^{1,2}

¹State Key Laboratory of Atmospheric Environment and Extreme Meteorology, Institute of Atmospheric Physics, Chinese Academy of Sciences, Beijing, China, ²College of Earth and Planetary Sciences, University of Chinese Academy of Sciences, Beijing, China

Particulate nitrate (pNO₃⁻) pollution persists over the North China Plain despite emission controls. We unravel a key mechanism: tall industrial stacks (≥210 m) release ammonia which, under strong winter oxidizing conditions, forms ammonium nitrate aloft. Utilizing a novel 3D high-resolution nitrate assimilation dataset and machine learning (XGBoost-SHAP), we tracked a major pollution event. Nitrate formed above 200 m accumulated in the nocturnal residual layer. Morning boundary layer development mixed this pollution downward, elevating surface concentrations by up to 35.5 µg m⁻³ within hours. Crucially, the Taihang and Yanshan Mountains south-westerly winds channeled, transporting the plume ~400 km. Downwind urban heating and enhanced oxidants during winter (including COVID-19-period anomalies) further amplified nitrate production within the boundary layer. This study establishes a complete 3D picture of elevated nitrate formation, transport, and mixing, highlighting the need for targeted controls on elevated industrial sources and cross-regional strategies.

KEYWORDS

particulate nitrate, data assimilation, elevated source, three-dimensional transport, atmospheric oxidation

1 Introduction

Particulate nitrate (pNO $_3$) constitutes a dominant and increasingly problematic component of fine particulate matter (PM $_{2.5}$) posing multifaceted environmental and public health challenges. As a key driver of haze formation, it significantly degrades air quality and visibility, particularly in densely populated and industrialized regions like Beijing (Sun et al., 2015; Li et al., 2018; Brender, 2020; Kong et al., 2025). Since the Chinese government launched the Air Pollution Prevention and Control Action Plan in 2013, national PM $_{2.5}$ levels have declined by roughly 30%–50% through 2018, thanks to stringent emission controls. However, nitrate in PM $_{2.5}$ did not decline in parallel with overall reductions in emissions. Instead, pNO $_3$ -concentrations increased during winter pollution episodes, particularly over the North China Plain, and gradually replaced sulfate as the predominant inorganic component of PM $_{2.5}$ (Zhai et al., 2021; Zhai et al., 2023; Geng et al., 2024; Zhang et al., 2024). Nitrate pollution not only reduces visibility but also poses risks of respiratory and cardiovascular diseases (Xiao et al., 2014). Furthermore,

nitrate aerosols affect climate by altering Earth's radiation budget through both direct and indirect mechanisms (Levy et al., 2013; Zhang, 2020; Pohlker et al., 2023). As a crucial secondary inorganic pollutant, the formation of pNO3 is associated with atmospheric reactive nitrogen concentrations and involves complex atmospheric chemical reactions (Lin et al., 2020; Ye et al., 2023; Ge et al., 2025). In China pNO₃ forms predominantly through two primary routes: the daytime gas-phase oxidation of nitrogen dioxide (NO2) by hydroxyl radicals (OH) and the nighttime heterogeneous hydrolysis of dinitrogen pentoxide (N2O5) on aerosol surfaces (Chen et al., 2018; Wang et al., 2018). Additional pathways include the partitioning of gaseous nitric acid (HNO₃) into particulate ammonium nitrate in the presence of excess ammonia (NH₃) (Wen et al., 2018), the reaction of nitrate radical (NO₃) with hydrocarbons at night in VOC-rich environments (Ng et al., 2017), and surface reactions on mineral dust under moderate to high relative humidity (RH) (Golay et al., 2022). Furthermore aqueous-phase reactions involving dissolved NO2 under high humidity conditions have been shown to contribute to pNO₃ formation in China (Zhang et al., 2022).

Regional transport plays a critical role in nitrate pollution (Chen et al., 2014; Chen et al., 2017; Yang et al., 2022), enabling the longrange movement of nitrate-containing pollutants and affecting areas far from their emission sources (Li et al., 2019; Qu et al., 2021). In China, pollutants originating in industrial zones can be transported to urban and rural regions where they degrade air quality and threaten public health as demonstrated by studies in the Pearl River Delta, where cross-regional transport accounted for a significant portion of particulate nitrate formation (Parveen et al., 2021; Qu et al., 2021). Additionally, mixing of pollutants from different areas leads to complex chemical interactions and amplification of nitrate formation (Yu et al., 2020; Zhang et al., 2021b). As one of the most severely polluted regions in China, the North China Plain (NCP) experiences intricate pollutant formation and transport mechanisms due to its complex topography and meteorological conditions (Quan et al., 2020; Liu et al., 2023). Modeling and observational research show that over 60% of PM_{2,5} mass in Beijing during haze events derives from non-local transport (Wu et al., 2021). Topographic features such as the Taihang Mountains influence pollutant distribution by trapping emissions on windward slopes and promoting downwind advection along the range, which leads to pollutant buildup in adjacent regions (Wang et al., 2010; Zhang et al., 2021a). Emissions from elevated sources under favorable meteorological conditions can travel long distances, making understanding nitrate transport critical for air pollution control (Wang et al., 2022). Recent GEOS-Chem modeling studies emphasize the influence of both domestic regional transport and transboundary transport from foreign anthropogenic sources on nitrate aerosol levels. The foreign contribution involves longdistance pollutant transport and enhanced nitrate production via chemical interactions with local emissions, underscoring the need for both domestic and international emission control strategies (Xu et al., 2023).

In this study, a significant high-altitude pNO₃ pollution event was observed over Beijing during winter. The analysis reveals that pollutants from elevated sources, such as industrial emissions, played a key role in the formation of nitrate pollution in the upper boundary layer. By examining the vertical evolution of

nitrate, we identified the critical factors affecting its concentration and investigated its three-dimensional transport and transformation mechanisms. These findings provide a solid scientific basis for a deeper understanding of the formation and control of regional atmospheric pollution.

2 Data and methods

2.1 Inorganic components data

High resolution hourly pNO₃-, pNH₄+, and pSO₄²concentrations were derived from the vertical aerosol data assimilation system NAQPMS PDAF v2.0 (Nested Air Quality Prediction Model System with the Parallel Data Assimilation Framework version 2.0). This chemical transport model (CTM)data assimilation framework employs a hybrid Kalman nonlinear ensemble transform filter (KNETF) to combine ensemble Kalman filter stability with nonlinear ensemble-transform capabilities (Nerger, 2021; Li et al., 2024). Assimilating both surface observations and lidar profiles produces physically consistent, observation constrained representations of vertical mixing, plume evolution and regional transport, which are essential for characterizing nitrate formation in the lower troposphere. The dataset covers the North China Plain at a horizontal resolution of 5 km and a vertical resolution of 50 m (40 layers within the lowest 2 km), providing higher spatial detail. This resolution supports detailed analysis of spatial evolution, vertical distribution and longrange transport of nitrate in the lower troposphere. Performance assessment used independent hourly measurements from 24 assimilation sites and 9 validation sites operated by the China National Environmental Monitoring Center. The assimilation achieved Pearson correlation coefficients (R) of at least 0.86, root mean square error (RMSE) of at most 3.23 µg m⁻³, mean absolute error (MAE) of no greater than 1.49 $\mu g\ m^{-3}$ and R^2 of at least 0.74 across all five PM_{2.5} components and R of at least 0.96 with R^2 of no less than 0.93 for nitrate, organic carbon and elemental carbon (Li et al., 2024). We selected 11th February 2021 for detailed analysis because a severe and abrupt pNO₃ pollution event occurred in the lower troposphere (300-500 m above ground level) over Beijing (Figure 1), mainly influenced by non-surface sources and vertical transport rather than local surface emissions. This event typifies the recurrent wintertime pollution episodes in northern China driven by southwesterly inflow and mountain-blocking effects (Zhu et al., 2011; Chang et al., 2018; Hu et al., 2022), providing a representative case for examining vertical pollutant transport processes.

2.2 Meteorological data

The vertical concentration data of NO_2 and ozone (O_3) were obtained from the Copernicus Atmosphere Monitoring Service (CAMS) global reanalysis (EAC4) monthly averaged fields (grid resolution 0.75 $^{\circ}$ × 0.75 $^{\circ}$, temporal resolution 3 h) (Inness et al., 2019), which were also used to calculate the atmospheric oxidizing capacity (AOC) as $NO_2 + O_3$. Meteorological variables including temperature (T), RH, wind components (UVW), and Planetary Boundary Layer Height (PBLH) were obtained from

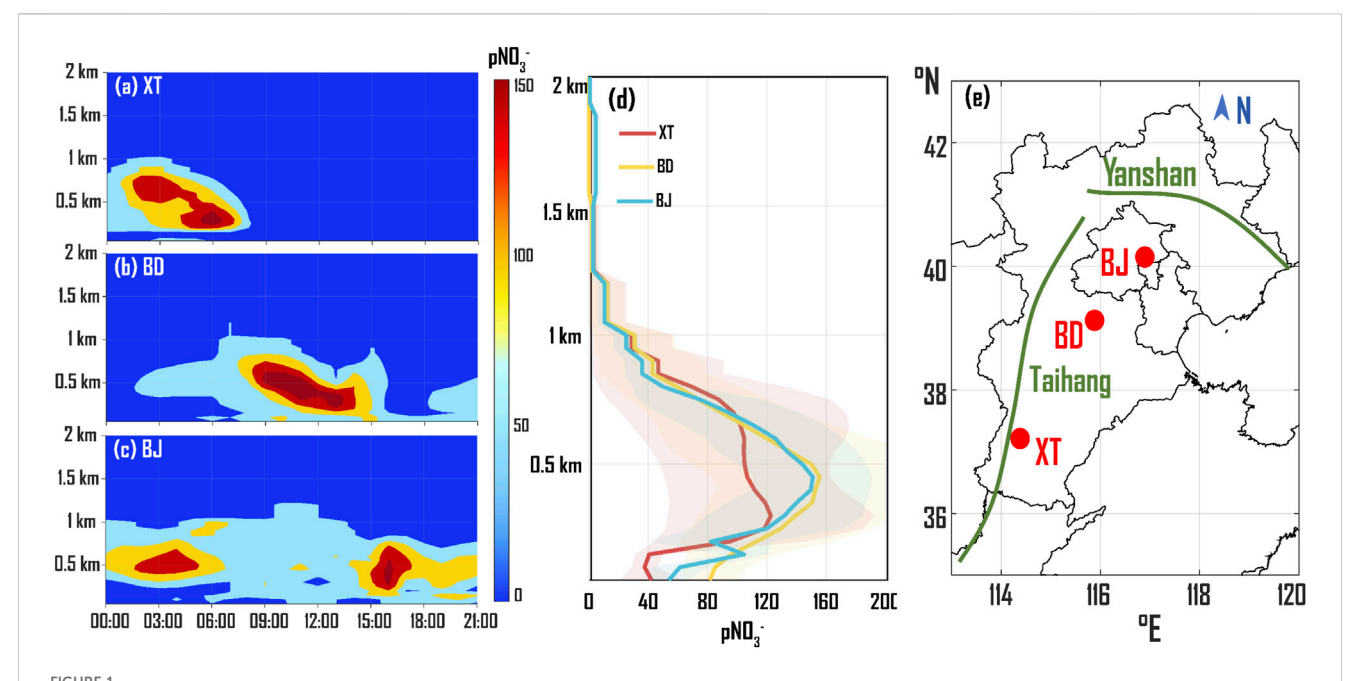


Figure 1 ($\mathbf{a} = \mathbf{c}$) Time-height cross-sections of pNO₃⁻ vertical distribution in the boundary layer for Xingtai, Baoding, and Beijing; (\mathbf{d}) Nitrate concentration profiles for each site during their prevailing periods. Units of pNO₃⁻ are μ g m⁻³; (\mathbf{e}) Locations of the three cities and surrounding topography, including the Taihang and Yanshan mountains.

ERA5 hourly data on pressure levels (grid resolution 0.25 ° \times 0.25 °, temporal resolution 1 h) (Hersbach et al., 2023), provided by the Copernicus Climate Change Service (C3S) Climate Data Store (CDS). The CAMS reanalysis data were interpolated to a 0.25° grid to ensure spatial consistency with the ERA5 meteorological fields. To assess the accuracy of this interpolation, we compared CAMS-derived NO2 and O3 concentrations with ground-based observations from national air quality monitoring stations located in Xingtai, Baoding, and Beijing (https://quotsoft.net/air/). The resulting correlation coefficients (0.61–0.87) demonstrate strong consistency between the two datasets (Supplementary Figure S1). The turbulent kinetic energy (TKE) is computed using the following equation:

$$TKE = 0.5 \times \left(\delta_u^2 + \delta_v^2 + \delta_w^2\right) \tag{1}$$

$$\delta_w^2 = \frac{1}{N-1} \sum_{i=1}^N (w_i - \bar{w})^2$$
 (2)

$$\delta_u^2 = \frac{1}{N-1} \sum_{i=1}^N (u_i - \bar{u})^2$$
 (3)

$$\delta_{\nu}^{2} = \frac{1}{N-1} \sum_{i=1}^{N} (\nu_{i} - \bar{\nu})^{2}$$
 (4)

Here, N represents the total number of data points, calculated by averaging the hourly data every 6 hours from 00:00 UTC on 8 February to 23:00 UTC on 15 February 2021 at 40 vertical levels, resulting in 1,280 samples in total (N = 1,280). These averaged data were then linearly interpolated back to hourly resolution to ensure consistency with other variables. w_i denotes the ith vertical wind velocity (m s⁻¹), while u_i (v_i) corresponds to the ith horizontal wind speed (m s⁻¹). Additionally, \bar{w} and \bar{u} (\bar{v}) represent the mean vertical and horizontal wind speeds (m s⁻¹), respectively. It should be noted that although TKE was initially

derived from the ERA5 wind field gradients following standard formulations, we no longer interpret it as a strict estimate of turbulent kinetic energy. Instead, it is regarded as a proxy indicator of atmospheric stability or vertical mixing potential, reflecting the ease of vertical exchange rather than the detailed turbulence structure. Due to its pronounced diurnal variability (Supplementary Figure S2), this parameter effectively captures variations in vertical mixing likelihood.

Due to the vertical extent limitations of reanalysis meteorological data, which do not reach the surface, we supplemented ground-level measurements using national air quality data from the China National Environmental Monitoring Center. This approach extended our study's vertical range from 50 to 2,000 m.

2.3 Methodology

XGBoost (eXtreme Gradient Boosting) and SHAP (SHapley Additive exPlanations) were used to quantify and interpret how meteorological and photochemical factors drive pNO₃⁻ at three Chinese sites (Xingtai, Baoding, Beijing) across different altitude layers ranging from 50 m to 2,000 m (Li, 2022; Jovanovic et al., 2023; Song et al., 2024). For each layer we constructed a feature matrix including T, RH, TKE, U, V, W, and AOC, then scaled them to the zero-to-one range. Supplementary Table S1 lists the exact input variables used in the XGBoost model, their symbols, units, and temporal resolutions. The data from February 11th, when elevated pollution was observed over Xingtai, Baoding, and Beijing, were used as the test set, whereas the full 8-day period from February 8th to 15th was used as the training set. The detailed training and testing

sample sizes for each layer and region are now provided in Supplementary Table S2. The number of training samples for Xingtai, Baoding, and Beijing is 1,152, 1920, 1,536, and 3,072, respectively, which is sufficient for robust model performance (Stirnberg et al., 2021). A gradient-boosted decision tree model was trained for 100 iterations with a maximum tree depth of five. During training, 80% of the samples and 80% of the features were randomly selected for each iteration. The model was optimized by minimizing the RMSE. We reported hold-out mean squared error (MSE) and applied a SHapley TreeExplainer to compute each predictor's contribution. The XGBoost model thereby quantified the relationship between nitrate concentrations and meteorological variables, while also assessing the importance of each factor. SHAP values were used to analyze the influence of these factors, providing insights into their spatial distribution and transport mechanisms. Because the assimilated concentration fields originate from CTM outputs, they inherently include both local and non-local influences, such as precursor transport. This integrated chemical transport model-machine learning (CTM-ML) architecture thus unites the mechanistic foundation of physically based modeling with the interpretability of explainable artificial intelligence, providing a robust framework for diagnosing the drivers of long-range nitrate transport and transformation over northern China.

3 Results and discussion

3.1 High-altitude transport process

Xingtai (XT), Baoding (BD), and Beijing (BJ) are three cities on the eastern foothills of the Taihang Mountains, which form the western boundary of the North China Plain (NCP). Xingtai lies in southern Hebei Province, bordering Shanxi Province to the west and the plain to the east. Baoding occupies central-western Hebei, encompassing both mountainous terrain and flatland at the mountain base. Western Beijing extends into the northern terminus of the Taihang range. Consequently, the Taihang Mountains act as a natural barrier that channels nitrate pollution from Xingtai through Baoding to Beijing, following a southwest-to-northeast trajectory (Figure 1e).

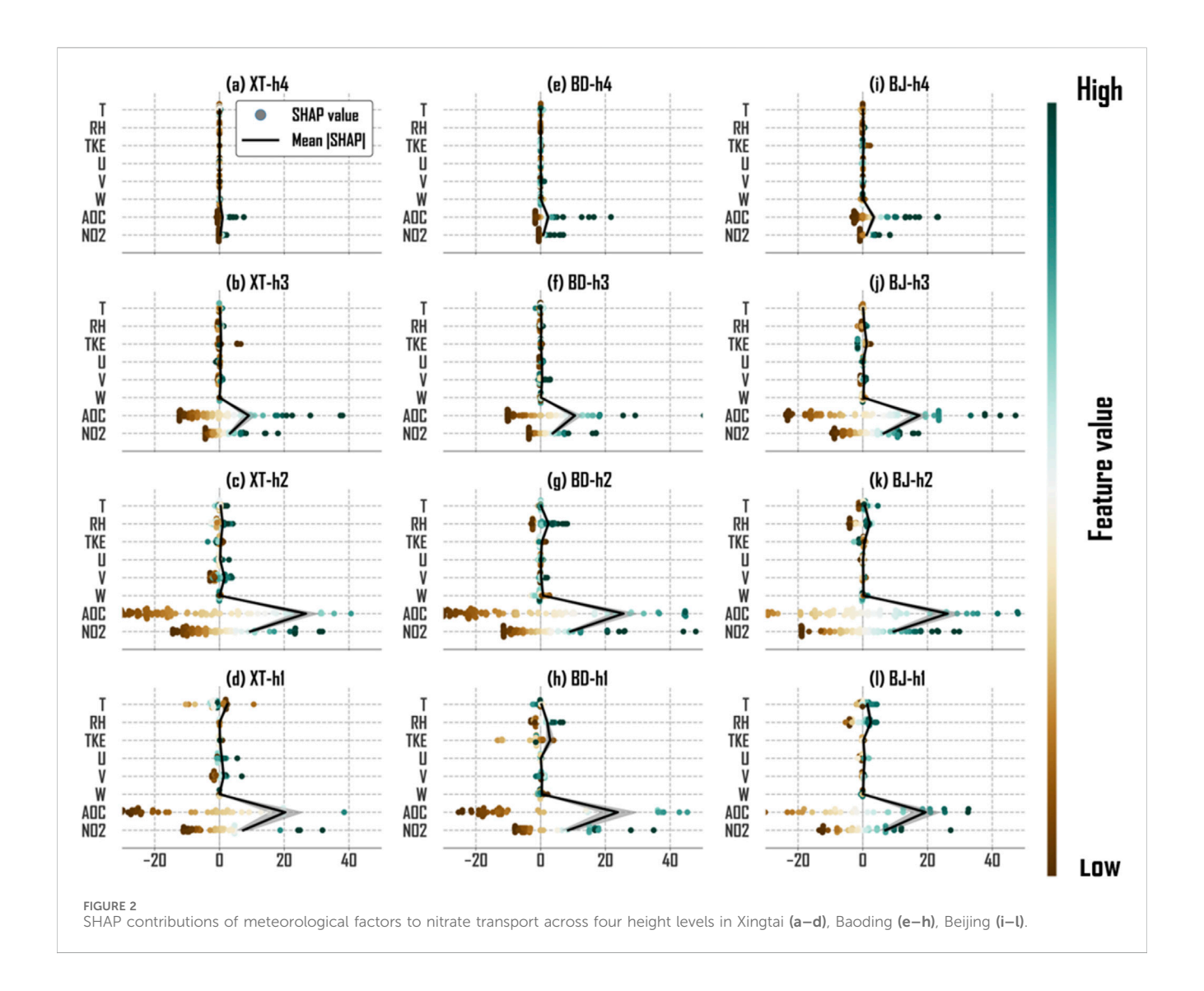
On 11 February 2021, a regional nitrate pollution episode was captured simultaneously at the three sites. In the early hours of 11 February 2021, a sudden increase in nitrate concentrations was detected in Xingtai at altitudes between 200 m and 800 m, with a peak concentration of 230.83 µg m⁻³ at 300 m (Figure 1a). This pollution episode persisted for approximately 6 hours. Between 09: 00 and 15:00 the same day, Baoding experienced a comparable event from the surface up to 800 m, with a maximum concentration of 265.57 μg m⁻³ at 450 m (Figure 1b). Later, between 16:00 and 18:00, a high-concentration nitrate plume was observed over Beijing between 200 m and 700 m, with a maximum concentration of 218.10 μg m⁻³ at 450 m (Figure 1c). This plume subsequently descended to the surface, leading to an increase in ground-level nitrate concentration by 35.45 µg m⁻³ within 2 hours. Beyond concentration evolution, meteorological analysis over Beijing further supports this transport pattern. As shown by the time series of horizontal wind components (Supplementary Figure S3), the westerly component remained weak due to the blocking effect of the Taihang Mountains, while the southerly component peaked before the nitrate maximum and then declined. This configuration suggests that southwesterly flows, after reaching northern Beijing and encountering the east–west-oriented Yanshan Mountains, were weakened and deflected, facilitating pollutant accumulation. Therefore, the February 11th episode provides a clear and representative case illustrating how complex mountain terrain modulates the transport and buildup of elevated nitrate pollution under typical winter conditions.

Accordingly, we defined the prevailing nitrate pollution periods on 11th February as 00:00 to 10:00 in Xingtai, 08:00 to 17:00 in Baoding and 15:00 to 19:00 in Beijing. During these intervals surface nitrate concentrations peaked highest in Baoding, followed by Beijing and Xingtai (Figure 1d). Within each prevailing period the peak occurred at the highest altitude in Baoding followed by Beijing and Xingtai. Peak nitrate concentrations also followed this order, reflecting the influence of multiple interacting factors. The time-shifted nitrate peaks from Xingtai to Baoding and Beijing correspond well to the sequential transport of the plume along the southwest-northeast corridor. Specifically, the slightly higher pollution altitude in Baoding indicates that the plume ascended adiabatically along the foothills of the Taihang Mountains under persistent southwesterly flow, and then descended near Beijing as the boundary layer deepened in the afternoon. This vertical motion influenced regional accumulation and the distribution of nitrate concentrations. AOC driven by NO₂ and O₃ enhanced conversion of precursors into pNO₃. Dynamic characteristics such as wind speed and transport patterns governed regional accumulation. High relative humidity and low temperatures during winter promoted nitrate partitioning into the particle phase, while regional emission intensity controlled the availability of precursors (Li et al., 2018; Chen et al., 2020; Zhang et al., 2024).

3.2 Driving factors of nitrate formation

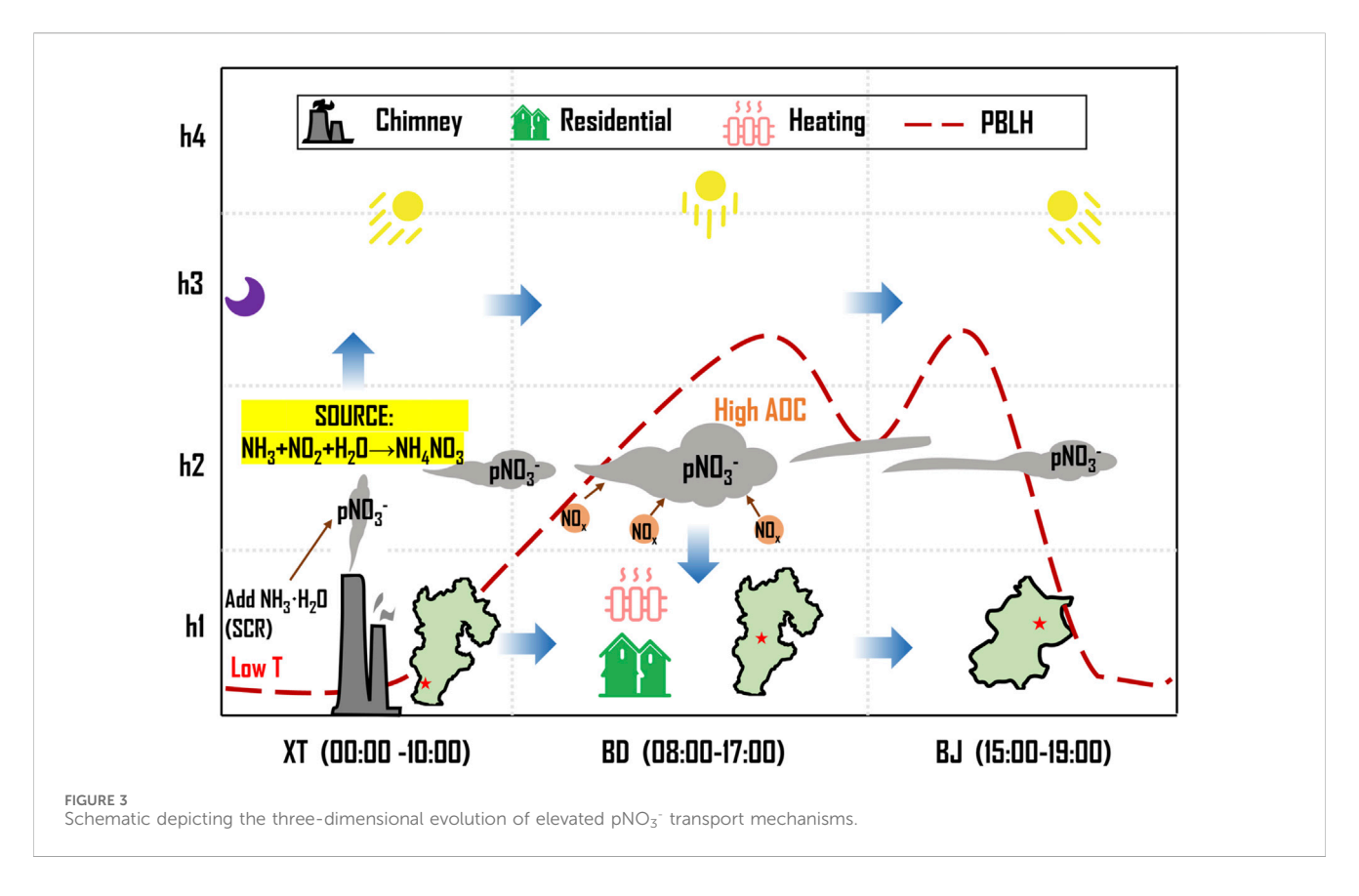
To characterize three dimensional nitrate transport in Xingtai, Baoding and Beijing at altitudes between 50 m and 2,000 m, we identified three key driving factors influencing nitrate concentrations: dynamic processes represented by UVW and TKE, thermodynamic processes represented by RH and T, and photochemical processes represented by AOC and NO₂ (Ge et al., 2017). Based on the vertical trends in Figure 1d we defined four height layers: h1 from 50 to 300 m, h2 from 300 to 800 m, h3 from 800 to 1,200 m and h4 from 1,200 to 2,000 m. Figure 2 presents a layer-by-layer analysis of pNO₃⁻ formation factors in each city.

pNO₃ pollution from elevated sources in Xingtai was transported towards Baoding and Beijing under increasing southwest winds (Supplementary Figure S4). In Xingtai below 300 m (h1), significant positive contributions of AOC and NO₂ to nitrate concentrations (mean |SHAP| >25, Figure 2d) indicated dominant photochemical formation. Lower temperatures further promoted nitrate formation. Westerly winds suggested nocturnal downslope flow from the Taihang Mountains, transporting cold, humid air masses that established shallow stable layers. A distinct 150 µg m⁻³ nitrate concentration peak at 300 m, exceeding surface levels and occurring under weak regional transport winds,



confirmed local elevated sources. Within 300-800 m (h2), high RH and updrafts supported nitrate formation via nocturnal heterogeneous reactions and vertical pollutant transport (Figure 2c). Upon reaching Baoding within h2, the influence of AOC and NO₂ intensified substantially (mean |SHAP| >40 and >15, respectively), exceeding contributions at other altitudes and along the pathway (Figure 2g). Pollution persistence for approximately 7 h, combined with low TKE, underscored the dominance of photochemistry and dynamical processes here. Within h1, southwesterly flow transported pollutants, while suppressed turbulence (negative TKE contribution) drove sharp increases in surface nitrate concentrations (Figure 2h). As the plume approached Beijing, terrain blocking by the Yanshan Mountains altered dynamics. Within h1, southerly winds became the primary positive contributor to near-surface nitrate, with markedly lower local photochemical influence compared to Xingtai (Figure 2l). This indicated Beijing's elevated ground-level nitrate predominantly from horizontal transport, not local production. Within h2, dynamical transport processes remain secondary only to photochemistry (Figure 2k). Above 800 m (h3 and higher), nitrate production in Xingtai, Baoding, and Beijing continued to be driven by AOC and was advected by southwesterly winds. However, the absolute contribution of AOC was markedly reduced owing to the sharp decline in nitrate concentrations at these heights (Figures 2a,b,e,f,i-k).

As shown in Figure 2, the SHAP values are relatively small for most predictors except AOC and NO2, which exhibit the largest contributions because they are directly linked to nitrate chemistry. This pattern is consistent with atmospheric chemical theory, as AOC reflects the oxidizing capacity of the atmosphere and NO₂ represents the abundance of its key precursor. The smaller SHAP values for other predictors indicate secondary but still meaningful influences on nitrate variability. It is important to note that our interpretation is not based solely on machine learning. The 3D structures of nitrate transport and vertical gradients were first identified from the assimilated NAQPMS-PDAF fields, and the ML SHAP analysis was then applied to quantify how meteorological and chemical conditions contributed to these observed features. Under this analytical framework, SHAP values express the relative, rather than absolute, influence of each predictor, allowing a mechanistic interpretation of how assimilated atmospheric states respond to key meteorological and photochemical processes.



3.3 Three-dimensional evolution mechanisms

pNO₃ pollution evolved through a three-dimensional mechanism involving elevated source generation, regional transport, enhanced atmospheric oxidation, and boundary layer processes, as illustrated in Figure 3. In Xingtai, coal-fired power plants utilized flue gas treatment systems including selective catalytic reduction (SCR) to ensure compliance with the Emission Standards for Air Pollutants from Coal-Fired Power Plants (Song et al., 2018; Li and Mao, 2020). During SCR operation, ammonia injection reacted with SO2 and nitrogen oxides (NO_x) to form ammonium sulfate and ammonium nitrate (Centi and Perathoner, 2007; Wang et al., 2023). However, following the nationwide implementation of ultra-low-emission retrofits, SO2 concentrations in flue gases have been substantially reduced. Under these conditions, the residual excess NH3 released from SCR units preferentially reacts with nitric acid (HNO₃) to form ammonium nitrate, rather than ammonium sulfate, leading to enhanced nitrate formation from elevated emission sources. (Terrenoire et al., 2022; Qi et al., 2023). This mechanism was supported by a very strong observed correlation between nitrate and ammonium ($r \approx 0.9$ on average across h1-h4), which was substantially higher than the correlation between nitrate and sulfate (Supplementary Figure S5). During winter nights, the elevated AOC and high RH significantly enhanced the nitrate concentration in the region. During nighttime, nitrate was predominantly formed via the reaction of NO₃ radicals with NO₂ to produce N2O5; under conditions of high ozone concentration that further boosted atmospheric oxidation, the formation of N2O5 is more efficient (Zhou, 2017). The low-temperature, high-humidity environment then favored the heterogeneous hydrolysis of N2O5 to produce HNO_3 , which subsequently underwent gas-to-particle conversion to form pNO_3 . (Liu et al., 2025). This mechanism produced high ammonium nitrate concentrations above the nocturnal boundary layer, accumulating within the residual layer. Morning diffusion (08:00–10:00 LT) transported this pollution to lower altitudes as the diagnosed planetary boundary layer height (PBLH) increased by approximately 350 m.

When the high-altitude pollution plume from Xingtai reached a residential area in Baoding, nitrate concentrations within h2 layer increased markedly and remained elevated for an extended period. Notably, this event occurred during the COVID-19 lockdown when AOC was substantially enhanced (Gettelman et al., 2021; Li et al., 2022). In addition, centralized heating and the extensive use of fireworks during the Spring Festival released large amounts of NO_x. Daytime boundary layer development mixed surface-emitted precursors to higher altitudes, amplified upper-level atmospheric oxidation and accelerated local photochemistry. This process intensified and sustained upper-level nitrate pollution. Gas-phase oxidation pathways, particularly OH radical reactions with NO2, dominated urban nitrate formation, exceeding contributions from other chemical mechanisms (Chen et al., 2020). Consequently, the enhanced atmospheric oxidizing environment in densely populated residential areas served as a key driver for nitrate generation in particulate matter, thereby intensifying nitrate pollution clusters across Baoding. Downward mixing of transported nitrate from elevated sources further exacerbated lower-level pollution.

The nitrate pollution plume continued its northeastward transport, reached Beijing by the evening of February 11th, and maintained elevated nitrate levels in the upper atmosphere over Beijing. Simultaneously, the deposition of the high-altitude pollution plume, coupled with the northeastward transport of a low-altitude pollution



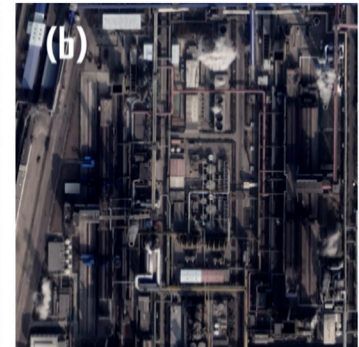




FIGURE 4
Satellite images of elevated point sources in Xingtai (a,b) and identification of anomalous hotspots in residential areas of Baoding (c)

plume originating from Baoding, further exacerbated surfacelevel pollution.

Based on the identified high-nitrate concentration regions, two elevated emission sources from power plants in Xingtai, whose chimneys reached up to 210 m, were located using Google Maps, as shown in Figures 4a,b. On $11^{\rm th}$ February 2021, an anomalous hotspot was detected over a residential area In Baoding (Figure 4c), supporting that nitrate produced by the elevated sources in Xingtai was enhanced over the Baoding residential zone and ultimately was transported to Beijing, thereby further corroborating the accuracy and reliability of the three-dimensional analysis of nitrate transport processes and mechanisms presented in this study.

4 Conclusion

Elevated industrial emissions from chimneys over 210 m released ammonia through SCR processes, which reacted with NO2 in the highly oxidative winter atmosphere to form pNO₃. The resulting nitrate-laden plumes entered the residual layer at night, where stable stratification and weak turbulence allowed for accumulation. After sunrise, convective mixing entrained this residual layer into the developing boundary layer, promoted vertical dispersion and extended surface influence. The Taihang and Yanshan mountain ranges acted as topographic barriers, guided the plume eastward over more than 385 km and affected air masses from the surface up to 1,200 m. In recent years, elevated atmospheric oxidants during winter, together with widespread residential heating and intensified fireworks emissions during the Spring Festival, enhanced nitrate formation in the lower and middle boundary layers. These nitrate-rich air masses were advected into downwind urban centers such as Beijing, elevated nocturnal nitrate levels and sustained pollution episodes. This study offers a detailed three-dimensional perspective on the formation and transport of elevated pNO3 across the North China Plain, thereby establishing a scientific basis for developing targeted, cross-regional strategies to control nitrate pollution and improve air quality.

Data availability statement

The raw data supporting the conclusions of this article will be made available by the authors, without undue reservation.

Author contributions

TY: Writing – original draft, Writing – review and editing. YT: Investigation, Software, Writing – original draft. ZW: Writing – review and editing.

Funding

The authors declare that financial support was received for the research and/or publication of this article. This work was supported by CAS Strategic Priority Research Program (XDB0760102), National Key Research and Development Program of China (grant no. 2023YFC3705801), National Natural Science Foundation of China (NSFC) Excellent Young Scientists Fund (grant no. 42422506), and the National Natural Science Foundation of China (grant no. 42275122).

Acknowledgements

We thank for the technical support of the National Large Scientific and Technological Infrastructure "Earth System Numerical Simulation Facility" (https://cstr.cn/31134.02.EL). Ting Yang would like to express gratitude towards the Program of the Youth Innovation Promotion Association (CAS).

Conflict of interest

The authors declare that the research was conducted in the absence of any commercial or financial relationships that could be construed as a potential conflict of interest.

Generative AI statement

The authors declare that no Generative AI was used in the creation of this manuscript.

Any alternative text (alt text) provided alongside figures in this article has been generated by Frontiers with the support of artificial intelligence and reasonable efforts have been made to ensure accuracy, including review by the authors wherever possible. If you identify any issues, please contact us.

Publisher's note

All claims expressed in this article are solely those of the authors and do not necessarily represent those of their affiliated

organizations, or those of the publisher, the editors and the reviewers. Any product that may be evaluated in this article, or claim that may be made by its manufacturer, is not guaranteed or endorsed by the publisher.

Supplementary material

The Supplementary Material for this article can be found online at: https://www.frontiersin.org/articles/10.3389/fenvs.2025.1718020/full#supplementary-material

References

Brender, J. D. (2020). "Human health effects of exposure to nitrate, nitrite, and nitrogen dioxide," in *Just enough nitrogen: perspectives on how to get there for regions with too much and too little nitrogen.* Editors M. A. Sutton, K. E. Mason, A. Bleeker, W. K. Hicks, C. Masso, and N. Raghuram (Cham: Springer International Publishing), 283–294

Centi, G., and Perathoner, S. (2007). "Chapter 1 introduction: state of the art in the development of catalytic processes for the selective catalytic reduction of NOx into N2," in *Studies in surface science and catalysis*. Editors P. Granger and V. I. Pârvulescu (Elsevier), 1–23.

Chang, X., Wang, S., Zhao, B., Cai, S., and Hao, J. (2018). Assessment of inter-city transport of particulate matter in the beijing-tianjin-hebei region. *Atmos. Chem. Phys.* 18 (7), 4843–4858. doi:10.5194/acp-18-4843-2018

Chen, T.-F., Chang, K.-H., and Tsai, C.-Y. (2014). Modeling direct and indirect effect of long range transport on atmospheric PM2.5 levels. *Atmos. Environ.* 89, 1–9. doi:10. 1016/j.atmosenv.2014.01.065

Chen, D., Liu, X., Lang, J., Zhou, Y., Wei, L., Wang, X., et al. (2017). Estimating the contribution of regional transport to PM2. 5 air pollution in a rural area on the North China plain. *Sci. Total Environ.* 583, 280–291. doi:10.1016/j.scitotenv.2017.01.066

Chen, Y., Wolke, R., Ran, L., Birmili, W., Spindler, G., Schröder, W., et al. (2018). A parameterization of the heterogeneous hydrolysis of N2O5 for mass-based aerosol models: improvement of particulate nitrate prediction. *Atmos. Chem. Phys.* 18 (2), 673–689. doi:10.5194/acp-18-673-2018

Chen, X., Wang, H., Lu, K., Li, C., Zhai, T., Tan, Z., et al. (2020). Field determination of nitrate formation pathway in winter beijing. *Environ. Sci. Technol.* 54 (15), 9243–9253. doi:10.1021/acs.est.0c00972

Ge, X., He, Y., Sun, Y., Xu, J., Wang, J., Shen, Y., et al. (2017). Characteristics and formation mechanisms of fine particulate nitrate in typical urban areas in China. *Atmosphere* 8 (3), 62. doi:10.3390/atmos8030062

Ge, M., Tong, S., Du, L., Wu, L., Lei, T., Li, K., et al. (2025). The influence of heterogeneous processes on the physicochemical properties of atmospheric aerosols. *Adv. Atmos. Sci.* 42 (4), 623–640. doi:10.1007/s00376-024-4077-y

Geng, G., Liu, Y., Liu, Y., Liu, S., Cheng, J., Yan, L., et al. (2024). Efficacy of China's clean air actions to tackle PM2.5 pollution between 2013 and 2020. *Nat. Geosci.* 17 (10), 987–994. doi:10.1038/s41561-024-01540-z

Gettelman, A., Chen, C. C., and Bardeen, C. G. (2021). The climate impact of COVID-19-induced contrail changes. *Atmos. Chem. Phys.* 21 (12), 9405–9416. doi:10.5194/acp-21-9405-2021

Golay, Z. M., Jones, S. H., and Donaldson, D. J. (2022). Reactive uptake of gas-phase NO2 by urban road dust in the dark. *ACS Earth Space Chem.* 6 (11), 2666–2672. doi:10. 1021/acsearthspacechem.2c00221

Hersbach, H., Bell, B., Berrisford, P., Biavati, G., Horányi, A., Muñoz Sabater, J., et al. (2023). ERA5 hourly data on pressure levels from 1940 to present. *Copernic. Clim. Change Serv.* (C3S) Atmos. Data Store. doi:10.24381/cds.bd0915c6

Hu, Q., Liu, C., Li, Q., Liu, T., Ji, X., Zhu, Y., et al. (2022). Vertical profiles of the transport fluxes of aerosol and its precursors between Beijing and its southwest cities. *Environ. Pollut.* 312, 119988. doi:10.1016/j.envpol.2022.119988

Inness, A., Ades, M., Agustí-Panareda, A., Barré, J., Benedictow, A., Blechschmidt, A. M., et al. (2019). The CAMS reanalysis of atmospheric composition. *Atmos. Chem. Phys.* 19 (6), 3515–3556. doi:10.5194/acp-19-3515-2019

Jovanovic, G., Perisic, M., Bacanin, N., Zivkovic, M., Stanisic, S., Strumberger, I., et al. (2023). Potential of coupling Metaheuristics-Optimized-XGBoost and SHAP in revealing PAHs environmental fate. *Toxics* 11 (4), 394. doi:10.3390/toxics11040394

Kong, L., Tang, X., Zhu, J., Wang, Z., Liu, B., Zhu, Y., et al. (2025). High-resolution simulation dataset of hourly PM2.5 chemical composition in China (CAQRA-aerosol) from 2013 to 2020. *Adv. Atmos. Sci.* 42 (4), 697–712. doi:10. 1007/s00376-024-4046-5

Levy, H., Horowitz, L. W., Schwarzkopf, M. D., Ming, Y., Golaz, J. C., Naik, V., et al. (2013). The roles of aerosol direct and indirect effects in past and future climate change. *J. Geophys. Res. Atmos.* 118 (10), 4521–4532. doi:10.1002/jgrd.50192

Li, Z. (2022). Extracting spatial effects from machine learning model using local interpretation method: an example of SHAP and XGBoost. *Comput. Environ. Urban Syst.* 96, 101845. doi:10.1016/j.compenvurbsys.2022.101845

Li, M., and Mao, C. (2020). Spatial effect of industrial energy consumption structure and transportation on haze pollution in beijing-tianjin-hebei region. *Int. J. Environ. Res. Public Health* 17 (15), 5610. doi:10.3390/ijerph17155610

Li, H., Zhang, Q., Zheng, B., Chen, C., Wu, N., Guo, H., et al. (2018). Nitrate-driven urban haze pollution during summertime over the North China plain. *Atmos. Chem. Phys.* 18 (8), 5293–5306. doi:10.5194/acp-18-5293-2018

Li, R., Mei, X., Wei, L., Han, X., Zhang, M., and Jing, Y. (2019). Study on the contribution of transport to PM2.5 in typical regions of China using the regional air quality model RAMS-CMAQ. *Atmos. Environ.* 214, 116856. doi:10.1016/j.atmosenv. 2019.116856

Li, L., Lu, C., Chan, P.-W., Lan, Z., Zhang, W., Yang, H., et al. (2022). Impact of the COVID-19 on the vertical distributions of major pollutants from a tower in the Pearl river Delta. *Atmos. Environ.* 276, 119068. doi:10.1016/j.atmosenv.2022.119068

Li, H., Yang, T., Nerger, L., Zhang, D., Zhang, D., Tang, G., et al. (2024). NAQPMS-PDAF v2.0: a novel hybrid nonlinear data assimilation system for improved simulation of PM2.5 chemical components. *Geosci. Model Dev.* 17 (23), 8495–8519. doi:10.5194/gmd-17-8495-2024

Lin, Y.-C., Zhang, Y.-L., Fan, M.-Y., and Bao, M. (2020). Heterogeneous formation of particulate nitrate under ammonium-rich regimes during the high-PM2.5 events in Nanjing, China. *Atmos. Chem. Phys.* 20 (6), 3999–4011. doi:10.5194/acp-20-3999-2020

Liu, J., Xue, L., Huang, X., Wang, Z., Lou, S., and Ding, A. (2023). Intensified haze formation and meteorological feedback by complex terrain in the North China plain region. *Atmos. Ocean. Sci. Lett.* 16 (2), 100273. doi:10.1016/j.aosl.2022.100273

Liu, Z., Qi, J., Ni, Y., Xue, L., and Liu, X. (2025). Enhanced atmospheric oxidation and particle reductions driving changes to nitrate formation mechanisms across coastal and inland regions of north China. Atmos. *Chem. Phys.* 2024. EGUsphere, 25 (15), 8719–8742. doi:10.5194/acp-25-8719-2025

Nerger, L. (2021). Data assimilation for nonlinear systems with a hybrid nonlinear Kalman ensemble transform filter. Q. J. R. Meteorological Soc. 148 (743), 620–640. doi:10.1002/qj.4221

Ng, N. L., Brown, S. S., Archibald, A. T., Atlas, E., Cohen, R. C., Crowley, J. N., et al. (2017). Nitrate radicals and biogenic volatile organic compounds: oxidation, mechanisms, and organic aerosol. *Atmos. Chem. Phys.* 17 (3), 2103–2162. doi:10. 5194/acp-17-2103-2017

Parveen, N., Siddiqui, L., Sarif, M. N., Islam, M. S., Khanam, N., and Mohibul, S. (2021). Industries in Delhi: air pollution versus respiratory morbidities. *Process Saf. Environ. Prot.* 152, 495–512. doi:10.1016/j.psep.2021.06.027

Pohlker, M. L., Pohlker, C., Quaas, J., Mulmenstadt, J., Pozzer, A., Andreae, M. O., et al. (2023). Global organic and inorganic aerosol hygroscopicity and its effect on radiative forcing. *Nat. Commun.* 14 (1), 6139. doi:10.1038/s41467-023-41695-8

Qi, L., Zheng, H., Ding, D., and Wang, S. (2023). Responses of sulfate and nitrate to anthropogenic emission changes in eastern China - in perspective of long-term variations. *Sci. Total Environ.* 855, 158875. doi:10.1016/j.scitotenv.2022.158875

Qu, K., Wang, X., Xiao, T., Shen, J., Lin, T., Chen, D., et al. (2021). Cross-regional transport of PM2.5 nitrate in the Pearl river Delta, China: contributions and mechanisms. *Sci. Total Environ.* 753, 142439. doi:10.1016/j.scitotenv.2020.142439

Quan, J., Dou, Y., Zhao, X., Liu, Q., Sun, Z., Pan, Y., et al. (2020). Regional atmospheric pollutant transport mechanisms over the North China plain driven by topography and planetary boundary layer processes. *Atmos. Environ.* 221, 117098. doi:10.1016/j.atmosenv.2019.117098

Song, X., Jiang, C., Lei, Y., Zhong, Y., and Wang, Y. (2018). Permitted emissions of major air pollutants from coal-fired power plants in China based on best available control technology. Front. Environ. Sci. & Eng. 12 (5), 11. doi:10.1007/s11783-018-1065-4

- Song, Z., Cao, S., and Yang, H. (2024). An interpretable framework for modeling global solar radiation using tree-based ensemble machine learning and Shapley additive explanations methods. *Appl. Energy* 364, 123238. doi:10.1016/j.apenergy.2024.123238
- Stirnberg, R., Cermak, J., Kotthaus, S., Haeffelin, M., Andersen, H., Fuchs, J., et al. (2021). Meteorology-driven variability of air pollution (PM1) revealed with explainable machine learning. *Atmos. Chem. Phys.* 21 (5), 3919–3948. doi:10.5194/acp-21-3919-2021
- Sun, Y. L., Wang, Z. F., Du, W., Zhang, Q., Wang, Q. Q., Fu, P. Q., et al. (2015). Long-term real-time measurements of aerosol particle composition in Beijing, China: seasonal variations, meteorological effects, and source analysis. *Atmos. Chem. Phys.* 15 (17), 10149–10165. doi:10.5194/acp-15-10149-2015
- Terrenoire, E., Hauglustaine, D. A., Cohen, Y., Cozic, A., Valorso, R., Lefèvre, F., et al. (2022). Impact of present and future aircraft $\mathrm{NO_x}$ and aerosol emissions on atmospheric composition and associated direct radiative forcing of climate. *Atmos. Chem. Phys.* 22 (18), 11987–12023. doi:10.5194/acp-22-11987-2022
- Wang, F., Chen, D. S., Cheng, S. Y., Li, J. B., Li, M. J., and Ren, Z. H. (2010). Identification of regional atmospheric PM10 transport pathways using HYSPLIT, MM5-CMAQ and synoptic pressure pattern analysis. *Environ. Model. & Softw.* 25 (8), 927–934. doi:10.1016/j.envsoft.2010.02.004
- Wang, H., Lu, K., Guo, S., Wu, Z., Shang, D., Tan, Z., et al. (2018). Efficient N2O5 uptake and NO3 oxidation in the outflow of urban Beijing. *Atmos. Chem. Phys.* 18 (13), 9705–9721. doi:10.5194/acp-18-9705-2018
- Wang, R., Wang, X., Cheng, S., Wang, K., Cheng, L., Zhu, J., et al. (2022). Emission characteristics and reactivity of volatile organic compounds from typical high-energy-consuming industries in North China. *Sci. Total Environ.* 809, 151134. doi:10.1016/j. scitotenv.2021.151134
- Wang, L., Zhou, S., You, M., Yu, D., Zhang, C., Gao, S., et al. (2023). Research progress on metal oxides for the selective catalytic reduction of NOx with ammonia. *Catalysts* 13 (7), 1086. doi:10.3390/catal13071086
- Wen, L., Xue, L., Wang, X., Xu, C., Chen, T., Yang, L., et al. (2018). Summertime fine particulate nitrate pollution in the North China plain: increasing trends, formation mechanisms and implications for control policy. *Atmos. Chem. Phys.* 18 (15), 11261–11275. doi:10.5194/acp-18-11261-2018
- Wu, J., Bei, N., Wang, Y., Li, X., Liu, S., Liu, L., et al. (2021). Insights into particulate matter pollution in the North China plain during wintertime: local contribution or regional transport? *Atmos. Chem. Phys.* 21 (3), 2229–2249. doi:10.5194/acp-21-2229-2021
- Xiao, S., Wang, Q. Y., Cao, J. J., Huang, R. J., Chen, W. D., Han, Y. M., et al. (2014). Long-term trends in visibility and impacts of aerosol composition on visibility impairment in Baoji, China. *Atmos. Res.* 149, 88–95. doi:10.1016/j.atmosres.2014.06.006

- Xu, J. W., Lin, J., Luo, G., Adeniran, J., and Kong, H. (2023). Foreign emissions exacerbate PM2.5 pollution in China through nitrate chemistry. *Atmos. Chem. Phys.* 23 (7), 4149–4163. doi:10.5194/acp-23-4149-2023
- Yang, S., Yuan, B., Peng, Y., Huang, S., Chen, W., Hu, W., et al. (2022). The formation and mitigation of nitrate pollution: comparison between urban and suburban environments. *Atmos. Chem. Phys.* 22 (7), 4539–4556. doi:10.5194/acp-22-4539-2022
- Ye, C., Zhou, X., Zhang, Y., Wang, Y., Wang, J., Zhang, C., et al. (2023). Synthesizing evidence for the external cycling of NOx in high-to low-NOx atmospheres. *Nat. Commun.* 14 (1), 7995. doi:10.1038/s41467-023-43866-z
- Yu, C., Zhao, T., Bai, Y., Zhang, L., Kong, S., Yu, X., et al. (2020). Heavy air pollution with a unique "non-stagnant" atmospheric boundary layer in the Yangtze river middle basin aggravated by regional transport of PM2.5 over China. *Atmos. Chem. Phys.* 20 (12), 7217–7230. doi:10.5194/acp-20-7217-2020
- Zhai, S., Jacob, D. J., Wang, X., Liu, Z., Wen, T., Shah, V., et al. (2021). Control of particulate nitrate air pollution in China. *Nat. Geosci.* 14 (6), 389–395. doi:10.1038/s41561-021-00726-z
- Zhai, S., Jacob, D. J., Pendergrass, D. C., Colombi, N. K., Shah, V., Yang, L. H., et al. (2023). Coarse particulate matter air quality in East Asia: implications for fine particulate nitrate. *Atmos. Chem. Phys.* 23 (7), 4271–4281. doi:10.5194/acp-23-4271-2023
- Zhang, B. (2020). The effect of aerosols to climate change and society. *J. Geoscience Environ. Prot.* 8 (08), 55–78. doi:10.4236/gep.2020.88006
- Zhang, J., Yuan, Q., Liu, L., Wang, Y., Zhang, Y., Xu, L., et al. (2021a). Trans-Regional transport of haze particles from the North China plain to Yangtze river Delta during winter. *J. Geophys. Res. Atmos.* 126 (8), e2020JD033778. doi:10.1029/2020JD033778
- Zhang, W., Hai, S., Zhao, Y., Sheng, L., Zhou, Y., Wang, W., et al. (2021b). Numerical modeling of regional transport of PM2.5 during a severe pollution event in the Beijing–Tianjin–Hebei region in November 2015. *Atmos. Environ.* 254, 118393. doi:10.1016/j.atmosenv.2021.118393
- Zhang, Y.-L., Zhang, W., Fan, M.-Y., Li, J., Fang, H., Cao, F., et al. (2022). A diurnal story of Δ 17O(\$\rm{NO}_{3}^{-}\$\$) in urban Nanjing and its implication for nitrate aerosol formation. *npj Clim. Atmos. Sci.* 5 (1), 50. doi:10.1038/s41612-022-00273-3
- Zhang, Z., Lu, B., Liu, C., Meng, X., Jiang, J., Herrmann, H., et al. (2024). Nitrate pollution deterioration in winter driven by surface ozone increase. *npj Clim. Atmos. Sci.* 7 (1), 160. doi:10.1038/s41612-024-00667-5
- Zhou, L. (2017). Atmospheric chemistry of NO₃: reactions with a series of organic and inorganic compounds.
- Zhu, L., Huang, X., Shi, H., Cai, X., and Song, Y. (2011). Transport pathways and potential sources of PM10 in Beijing. *Atmos. Environ.* 45 (3), 594–604. doi:10.1016/j. atmosenv.2010.10.040